Image Analysis Using Hahn Moments

Pew-Thian Yap,
Raveendran Paramesran, *Sr. Member*, *IEEE*,
and Seng-Huat Ong

Abstract—This paper shows how Hahn moments provide a unified understanding of the recently introduced Chebyshev and Krawtchouk moments. The two latter moments can be obtained as particular cases of Hahn moments with the appropriate parameter settings and this fact implies that Hahn moments encompass all their properties. The aim of this paper is twofold: 1) To show how Hahn moments, as a generalization of Chebyshev and Krawtchouk moments, can be used for global and local feature extraction and 2) to show how Hahn moments can be incorporated into the framework of normalized convolution to analyze local structures of irregularly sampled signals.

Index Terms—Hahn polynomials, Hahn moments, discrete orthogonal polynomials, normalized convolution.

1 Introduction

THE notion of *discrete orthogonal moments* was introduced by Mukundan et al. [1]. In their paper, the set of Chebyshev moments was proposed and utilized for image analysis and the advantages of this particular set of moments are: 1) no numerical approximation is needed in computing the moments since their moment kernels are polynomials of discrete variables, i.e., discrete Chebyshev polynomials [1] and 2) no spatial domain normalization is required due to the fact that the domain of the polynomials matches the discrete domain of the image.

Taking the cue from Mukundan et al.'s work, we introduced the set of Krawtchouk moments [2]. Krawtchouk moments, like Chebyshev moments, belong to the class of *discrete orthogonal moments*. However, Krawtchouk moments are local descriptors; this is different from Chebyshev moments which are global descriptors. By the term *global*, it is meant that the features are extracted from the image as a whole, i.e., giving equal emphasis to all the pixels in the image. On the contrary, the term *local* means that the features extracted are from only a particular portion of the image, i.e., more emphasis is given to a certain portion or region of the image.

The concern of this paper is to show how Hahn moments [3], [4], [5] provide a unified understanding of Chebyshev and Krawtchouk moments, and how this point can be exploited and utilized in the context of image analysis. The set of Hahn moments becomes Chebyshev moments or Krawtchouk moments depending on how the parameters $\{\alpha_1, \beta_1, \alpha_2, \beta_2\}$ are set, i.e., Chebyshev and Krawtchouk moments are particular cases of Hahn moments. A direct implication of this fact is that Hahn moments encompass all the properties of both Chebyshev and Krawtchouk moments, and Hahn moments, in addition, also exhibit intermediate properties between the extremes set by Chebyshev and Krawtchouk moments.

- *P.-T. Yap is with the School of Electrical and Electronic Engineering, Nanyang Technological University, Singapore 639798. E-mail: pewthian@ntu.edu.sg.*
- *R. Paramesran is with the Department of Electrical Engineering, Faculty of Engineering, University of Malaya, 50603 Kuala Lumpur, Malaysia. E-mail: ravee@um.edu.my.*
- *S.-H. Ong is with the Institute of Mathematical Sciences, Faculty of Science, University of Malaya, 50603 Kuala Lumpur, Malaysia. E-mail: ongsh@um.edu.my.*

Manuscript received 3 June 2006; revised 2 Feb. 2007; accepted 14 May 2007; published online 31 May 2007.
Recommended for acceptance by P. Maragos.
For information on obtaining reprints of this article, please send e-mail to: tpami@computer.org, and reference IEEECS Log Number TPAMI-0544-0706.
Digital Object Identifier no. 10.1109/TPAMI.2007.70709.

This makes Hahn moments a unique set of feature descriptors in their own right. This paper aims to highlight the generalization property of Hahn moments and to show how this property can be properly exploited to make Hahn moments a useful set of image feature descriptors.

The accuracy of Hahn moments as descriptors is assessed by means of image reconstruction. By inspecting the image reconstructed from its set of moments, one can determine the number of moments required to capture the essential characteristics of the image. To illustrate the global feature extraction capability of Hahn moments, images are reconstructed with Hahn, Chebyshev, Zernike, and Legendre moments, and their respective results are presented. To demonstrate the local feature extraction capability, it is shown how Hahn moments can be used to extract features from different locations of an image. To further demonstrate this point, a simple adaptive image reconstruction scheme is presented to show how the parameters of Hahn moments can be selected adaptively based on the image characteristics. The results of these experiments collectively show that Hahn moments give positive improvements and has added advantage over the other moments in consideration.

To further demonstrate the usefulness of Hahn moments, it is also shown how Hahn moments can be incorporated into the framework of normalized convolution [6] to analyze local structures of irregularly sampled signals. This is built upon the fact that the set of Hahn polynomials [7] spans a weighted space defined by the related weight function, which for the case of Hahn polynomials resembles the Gaussian function. The weight function serves as a windowing function which gives higher importance to points at the center of the neighborhood than points farther away, i.e., the weight function decreases monotonically toward its tails. Hahn polynomials provide an orthogonal basis in this weighted space, making analysis a little easier when compared to nonorthogonal basis.

2 Mathematical Background

We first list here some notations and definitions which will be useful later.

2.1 Notations and Definitions

Definition 2.1 (Pochhammer symbol). *The Pochhammer symbol is defined as*

$$(a)_k = a(a+1)(a+2)\ldots(a+k-1), \tag{1}$$

where $k = 1, 2, 3, \ldots$ *and* $(a)_0 = 1$.

Definition 2.2 (Hypergeometric series).

$${}_rF_s\left(\begin{matrix} a_1, \ldots, a_r \\ b_1, \ldots, b_s \end{matrix}\middle| z\right) = \sum_{k=0}^{\infty} \frac{(a_1, \ldots, a_r)_k}{(b_1, \ldots, b_s)_k} \frac{z^k}{k!}, \tag{2}$$

where $(a_1, \ldots, a_r)_k = (a_1)_k, \ldots, (a_r)_k$ *and*

$$(b_1, \ldots, a_s)_k = (b_1)_k, \ldots, (b_s)_k.$$

Definition 2.3 (Orthogonality condition). *For a set of discrete orthogonal polynomials* $\{v_n(x)\}$, n, $x = 0, 1, \ldots, N$, *with weight* $w(x)$ *and norm* $\rho(n)$, *we have orthogonality condition*

$$\sum_{x=0}^{N} w(x) v_m(x) v_n(x) = \rho(n)\delta_{mn}. \tag{3}$$

Definition 2.4 (Weighted polynomials). *For* weighted *polynomials, distinguished with an overline and defined as*

$$\overline{v}_n(x) = \left[\frac{w(x)}{\rho(n)}\right]^{\frac{1}{2}} v_n(x), \tag{4}$$

TABLE 1
Discrete Orthogonal Moments and Their Respective Kernels, Weights, Norms, and Parameters

Moments	Kernels	Weight, $w(x)$	Norm, $\rho(n)$	Parameters
Chebyshev Moments T_{mn}	$t_n(x;N) = {}_3F_2\left(\begin{array}{c} -n,-x,1+n \\ 1,-N \end{array}\middle\vert 1\right)$	$w(x;N) = \frac{1}{N+1}$	$\rho(n;N) = \frac{(2n)!}{N+1}\binom{N+n+1}{2n+1}$	–
Krawtchouk Moments K_{mn}	$k_n(x;p,N) = {}_2F_1\left(\begin{array}{c} -n,-x \\ -N \end{array}\middle\vert \frac{1}{p}\right)$	$w(x;p,N) = \binom{N}{x}p^x(1-p)^{N-x}$	$\rho(n;p,N) = \frac{(-1)^n n!}{(-N)_n}\left(\frac{1-p}{p}\right)^n$	$0<p<1$
Hahn Moments H_{mn}	$h_n(x;\alpha,\beta,N) = {}_3F_2\left(\begin{array}{c} -n,n+\alpha+\beta+1,-x \\ \alpha+1,-N \end{array}\middle\vert 1\right)$	$w(x;\alpha,\beta,N) = \binom{\alpha+x}{x}\binom{\beta+N-x}{N-x}$	$\rho(n;\alpha,\beta,N) = \frac{(-1)^n(n+\alpha+\beta+1)_{N+1}(\beta+1)_n n!}{(2n+\alpha+\beta+1)(\alpha+1)_n(-N)_n N!}$	$\alpha>-1$ & $\beta>-1$ or $\alpha<-N$ & $\beta<-N$

we have an orthogonal system

$$\sum_{x=0}^{N}\overline{v}_m(x)\overline{v}_n(x) = \delta_{mn} \tag{5}$$

and it is simple to prove that: $|\overline{v}_n(x)| \le 1$.

Definition 2.5 (Discrete moments). *The discrete moment of order $(m+n)$ of a two-dimensional image with intensity function $f(x,y)$,*[1] *$x \in \mathbf{S}_{M-1}$, $y \in \mathbf{S}_{N-1}$, $\mathbf{S}_k = \{0,1,2,\ldots,k\}$ is defined as*

$$\Psi_{mn} = \sum_{x=0}^{M-1}\sum_{y=0}^{N-1}\Phi_{mn}(x,y)f(x,y), \tag{6}$$

where $\Phi_{mn}(x,y)$, $m \in \mathbf{S}_{M-1}$, and $n \in \mathbf{S}_{N-1}$, are the moment kernel *or* basis function *of the moment. If the moment kernels are mutually orthogonal, we call the moments* discrete orthogonal moments. *In cases where the kernel is* separable, *we can express the kernel in two separate terms*

$$\Phi_{mn}(x,y) = \phi_m(x)\phi_n(y). \tag{7}$$

If the basis set is complete, *the image is completely characterized by the total of $M \times N$ moments.*

Definition 2.6 (Image reconstruction). *The image intensity function, $f(x,y)$, can be reconstructed easily by the linear combination of the set of moments, $\{\Psi_{mn}\}$, i.e.,*

$$f(x,y) = \sum_{m=0}^{M-1}\sum_{n=0}^{N-1}\Psi_{mn}\Phi_{mn}(x.y). \tag{8}$$

If the order of $\{\Psi_{mn}\}$ is limited to $m \le m_{\max}$, $n \le n_{\max}$, where $m_{\max} \le M-1$ and $n_{\max} \le N-1$, $\hat{f}(x,y)$ is an approximation of $f(x,y)$

$$\hat{f}(x,y) \simeq \sum_{m=0}^{m_{\max}}\sum_{n=0}^{n_{\max}}\Psi_{mn}\Phi_{mn}(x,y). \tag{9}$$

The quadratic error related to this approximation is

$$\epsilon^2(\hat{f}) = \sum_{x=0}^{M-1}\sum_{y=0}^{N-1}\left[\hat{f}(x,y) - f(x,y)\right]^2 \tag{10}$$

$$= \sum_{x=0}^{M-1}\sum_{y=0}^{N-1}[f(x,y)]^2 - \sum_{m=0}^{m_{\max}}\sum_{n=0}^{n_{\max}}[\Psi_{mn}]^2. \tag{11}$$

If the maximum order of $\{\Psi_{mn}\}$ is restricted to $(m+n) \le P$, where $P \le M+N-2$, we have

$$\hat{f}(x,y) \simeq \sum_{m=0}^{P}\sum_{n=0}^{m}\Psi_{m-n,n}\Phi_{m-n,n}(x,y) \tag{12}$$

and the error related to this approximation is

$$\epsilon^2(\hat{f}) = \sum_{x=0}^{M-1}\sum_{y=0}^{N-1}[f(x,y)]^2 - \sum_{m}^{P}\sum_{n=0}^{m}\left[\Psi_{m-n,n}\right]^2. \tag{13}$$

1. For the sake of simplicity, the discrete image intensity function $f(x_i, y_j)$ is denoted as $f(x,y)$.

3 Chebyshev, Krawtchouk, and Hahn Moments

3.1 Definitions

Chebyshev, Krawtchouk, and Hahn moments all have discrete orthogonal polynomials as their moment kernels. Table 1 gives a summary of the polynomials, the weights by which the polynomials can be derived from monomials using Gram-Schmidt orthogonalization [8], the norms, and also the parameters available for each. Note that, in formulating the moments, we use the weighted versions of the polynomials and this would give greater numerical stability as shown in [2]. The polynomials are used in a separable sense as shown in (7) and for each dimension, one set of polynomials is used. All the polynomials have support $x = 0,1,\ldots,N$.

3.2 Connection of Hahn Moments with Chebyshev and Krawtchouk Moments

The weighted Hahn, Krawtchouk, and Chebyshev polynomials are interrelated. If we take $\alpha = pt$ and $\beta = (1-p)t$ (hence, $p = \alpha/(\alpha+\beta)$, $t = \alpha+\beta$) in weighted Hahn polynomials and let $t \to \infty$, we obtain the weighted Krawtchouk polynomials

$$\lim_{t\to\infty}\overline{h}_n(x;\alpha,\beta,N) = \overline{k}_n(x;p,N). \tag{14}$$

If we let $t \to 0$ or simply let $\alpha = \beta = 0$, we obtain the weighted Chebyshev polynomials

$$\lim_{t\to 0}\overline{h}_n(x;\alpha,\beta,N) = \overline{t}_n(x). \tag{15}$$

Therefore, the weighted Hahn polynomials are generalizations of weighted Krawtchouk and Chebyshev polynomials. This is shown in

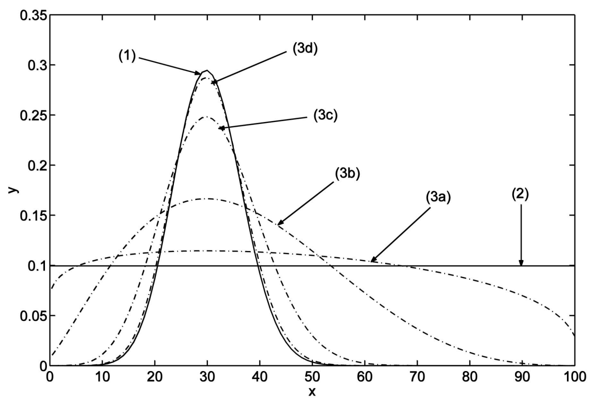

Fig. 1. The relationship between weighted Hahn, Krawtchouk, and Chebyshev polynomials. (1) Weighted Krawtchouk polynomial with $p = 0.3$, (2) Weighted Chebyshev polynomial, (3a) Weighted Hahn polynomial with $\alpha = 0.3$, $\beta = 0.7$, (3b) $\alpha = 3$, $\beta = 7$, (3c) $\alpha = 30$, $\beta = 70$, and (3d) $\alpha = 300$, $\beta = 700$. For all cases, $n = 0$. Since $t_0(x;N) = k_0(x;p,N) = h_0(x;\alpha,\beta,N) = 1$, the lines shown are in fact scaled versions of the square roots of the respective weight functions.

Fig. 1 for the zeroth order ($n = 0$). As can be seen from the figure, the weighted Hahn polynomial become increasingly like the weighted Krawtchouk polynomial when (14) is observed and, on the other hand, the weighted Chebyshev polynomial when (15) is observed. The proofs for (14) and (15) can be found in [4]. Hahn moments in connection with Chebyshev and Krawtchouk moments observe an identical relationship, but since Hahn moments cater for 2D images, we have two times the number of parameters: $\{\alpha_1, \beta_1, \alpha_2, \beta_2\}$.

3.3 Global-Local Tradeoff

It should be noted here that the Chebyshev polynomials are in fact *global* while Krawtchouk polynomials are *local*, as can be seen from Fig. 1. Notice that the values of Chebyshev polynomials are distributed throughout the whole range of x for all cases as shown in Fig. 1. Krawtchouk polynomials, on the other hand, have distributed values, position of which, as we shall see later, can be controlled by the parameter p. Following the discussion in the previous section, we can see that Hahn polynomials and, hence, their moments become more local when the value of t is increased, and on the other end, more global when t is closer to zero. It can be proven that, if $t \gg 2N$ (hence, we can set $t = 20N$), we can obtain a sufficiently close approximation.

3.4 Gaussian Approximation

For Np, $N(1-p) > 5$, and $t \to \infty$, the weight function of Hahn polynomials with parameters $\alpha = pt$ and $\beta = (1-p)t$ approximates the Gaussian function.[2] This follows from the fact that when $t \to \infty$ the weight function of Hahn polynomials approximates that of Krawtchouk polynomials (scaled by a multiplicative factor), which in turn is the probability mass function (PMF) of a binomial distribution (see Table 1 for the case of Krawtchouk polynomials), and it is well known that the PMF of a binomial distribution approximates the probability density function (PDF) of a Gaussian distribution when Np, $N(1-p) > 5$. The approximated Gaussian distribution has mean[3] $\mu = Np$ and variance $\sigma^2 = Np(1-p)$.

3.5 Hypergeometric Distribution Approximation

It can be shown that for integer values of α, β and if $\alpha, \beta \gg N$, the weight function of Hahn polynomials approximates the PMF of a hypergeometric distribution [9]. This can be shown by noting that

$$w(x;\alpha,\beta,N) \approx \binom{\alpha}{x}\binom{\beta}{N-x} = \binom{\alpha}{x}\binom{t-\alpha}{N-x}, \tag{16}$$

where $t = \alpha + \beta$. The PMF of hypergeometric distribution can be obtained by dividing the results with $\binom{t}{N}$. The hypergeometric distribution has some properties which can be used to help better select the values of α and β: mean $\mu = \frac{\alpha N}{\alpha+\beta}$, mode $\lfloor\frac{(\alpha+1)(N+1)}{\alpha+\beta+2}\rfloor$, and variance $\sigma^2 = \frac{\alpha\beta(\alpha+\beta-N)N}{(\alpha+\beta)^2(\alpha+\beta-1)}$. Since α, $\beta \gg N$, the mode and the variance can be approximated as $\lfloor\frac{\alpha(N+1)}{\alpha+\beta}\rfloor$ and $\frac{\alpha\beta N}{(\alpha+\beta)^2}$, respectively.

3.6 Parameter Selection

The region of emphasis of Hahn moments can be controlled by the parameters[4] $\alpha_1 = p_1 t_1$, $\beta_1 = (1-p_1)t_1$, and $\alpha_2 = p_2 t_2$, $\beta_2 = (1-p_2)t_2$. From the above discussion, we have seen that the weight function of Hahn polynomials approaches the PDF of a Gaussian distribution and hypergeometric distribution under different conditions. One important thing to note is that the means and modes of these two distributions have the value[5] $pN = \frac{\alpha N}{\alpha+\beta}$. It can in fact be proven[6] that the weight function of Hahn polynomials peaks at $\lfloor\frac{\alpha(N+1)}{\alpha+\beta}\rfloor$. We can utilize this fact to select the parameters of Hahn moments by first selecting $p_1 = x_c/N$ and $p_2 = y_c/N$ based on the center (x_c, y_c) of the intended region of emphasis and then setting $\alpha_1 = p_1 t_1$, $\beta_1 = (1-p_1)t_1$ and $\alpha_2 = p_2 t_2$, $\beta_2 = (1-p_2)t_2$; the parameters t_1 and t_2 are determined in a global-local tradeoff fashion as discussed in Section 3.3, the different values of t_1 and t_2 permit information to be extracted from the image in either a global or local sense. When α, $\beta \gg N$, the smallest area of coverage of Hahn moments is roughly[7] the box whose edges are of two standard deviations from the center (x_c, y_c), i.e., the box $(x_c - 2\sigma_1, x_c + 2\sigma_1) \times (y_c - 2\sigma_2, y_c + 2\sigma_2)$, where

$$\sigma_k = \left[\frac{\alpha_k \beta_k N}{(\alpha_k + \beta_k)^2}\right]^{1/2} = [p_k(1-p_k)N]^{1/2}.$$

4 Experimental Studies

4.1 Global Feature Extraction

Hahn moments can be set into global feature extraction mode by setting $\alpha_1 = \beta_1 = \alpha_2 = \beta_2 = 0$. In this experiment, the Hahn moments of the image are first calculated and, subsequently, their image representation power is verified by reconstructing the image from the moments and measuring the difference between the original image and the reconstructed image using the Mean Squared Error (MSE). A set of 100 test images are selected from different categories of the WBIIS [10] database. The images are converted to gray-scale format and are each resized to $M \times N = 128 \times 128$. A sample image and its reconstructed versions using Hahn moments are shown in Fig. 2. The average MSE values for Hahn moments (which are equivalent to Chebyshev moments in this case), Legendre moments [11], and Zernike moments[8] [11], up to order P (see (12)), are shown in Fig. 3. Note that the reconstruction error decreases monotonically with the increase of the order as predicted by (13). When compared to other moments, the results of Hahn

2. There are other criteria to determine whether the binomial distribution approximates the Gaussian distribution well enough, but we have chosen this one for simplicity.

3. The mode and the median share the same value with the mean.

4. We restrict our discussion to cases where α_1, β_1, α_2, and $\beta_2 \geq 0$.

5. The term 1 in $\lfloor\frac{\alpha(N+1)}{\alpha+\beta}\rfloor$ can be taken as a continuity correction term and its effect diminished as N increases, i.e., $\frac{\alpha(N+1)}{\alpha+\beta} \approx \frac{\alpha N}{\alpha+\beta}$.

6. By considering the fact that the weight function $w(x)$ is maximum at point x with $w(x)/w(x-1) \geq 1$ and $w(x+1)/w(x) \leq 1$.

7. The coverage grows as the order increases.

8. The images are mapped inside the unit circle.

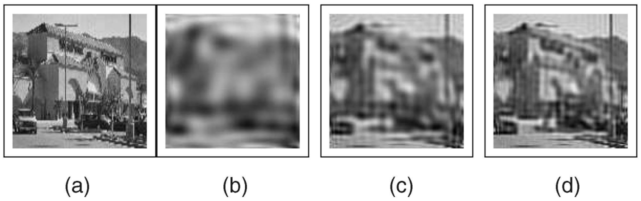

Fig. 2. Global feature extraction using Hahn moments. (a) Original. (b) $P = 20$. (c) $P = 40$. (d) $P = 60$.

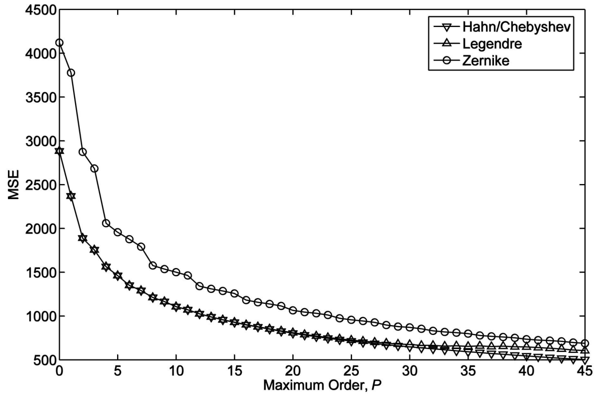

Fig. 3. MSE comparison of images reconstructed using Hahn/Chebyshev, Legendre, and Zernike moments, respectively.

moments are generally better. The similarity of results between Hahn (hence, Chebyshev) and Legendre moments is not surprising and has in fact been explained in [1].

4.2 Local Feature Extraction

Hahn moments can be set into local feature extraction mode by setting the parameters $\{\alpha_1, \beta_1, \alpha_2, \beta_2\} > 0$. Details on how to set the parameters of Hahn moments have been provided in Section 3.6. Fig. 4 shows the reconstruction results of the image Fig. 4a, where the four different aircrafts are located at the four different quadrants of the 128×128 image. Notice that only the features of the location specified by the respective settings of parameters $\{\alpha_1, \beta_1, \alpha_2, \beta_2\}$ are extracted, as verified by the reconstructed images in Figs. 4e, 4f, 4g, and 4h. Figs. 4b, 4c, and 4d show the reconstructed images when Hahn moments are set to global mode (i.e., $\{\alpha_1, \beta_1, \alpha_2, \beta_2\} = 0$). Notice that, in these cases, a larger number of moments are needed to extract the characteristics of the original image. Figs. 4i, 4j 4k, and 4l show the Hahn moment kernels for $m = n = 1$ at different positions as determined by the parameters.

4.3 Adaptive Feature Extraction

In this section, we show how the set of Hahn moments can be utilized to adaptively capture information of an image. By reconstructing the image from the moments, it is shown that the error of the reconstructed image under this adaptive scheme is reduced. In order to capture the features of an image adaptively, the parameters $\{\alpha_1, \beta_1, \alpha_2, \beta_2\}$ are set accordingly to the characteristics of the image. We choose

$$\alpha_1(f) = x_c t_1(f), \quad \beta_1(f) = (1 - x_c) t_1(f), \tag{17}$$

$$\alpha_2(f) = y_c t_2(f), \quad \beta_2(f) = (1 - y_c) t_2(f), \tag{18}$$

where $(x_0, y_0) \in [0, 1] \times [0, 1]$ is the normalized centroid

$$x_c = \frac{1}{M-1} \left(\sum_{x=0}^{M-1} \sum_{y=0}^{N-1} x f(x,y) \right) \left(\sum_{x=0}^{M-1} \sum_{y=0}^{N-1} f(x,y) \right)^{-1}, \tag{19}$$

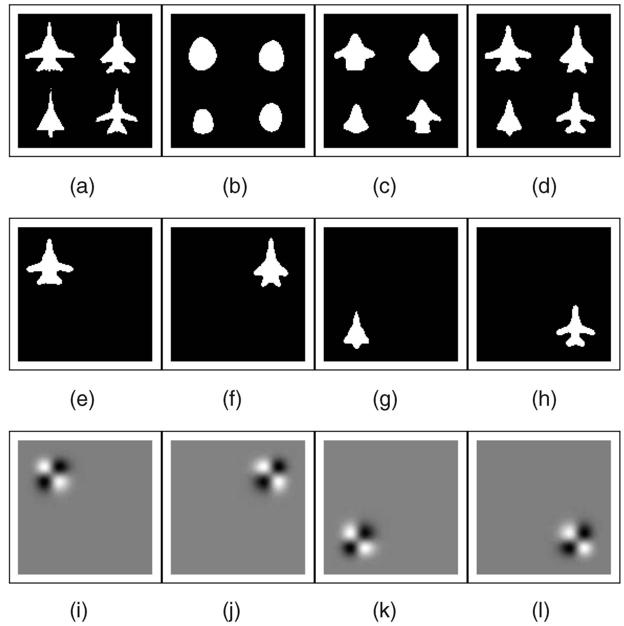

Fig. 4. Each individual aircraft can be extracted from the combined image (a), size 128×128, by setting the values of α_1, β_1, α_2, β_2 to: (e) $\alpha_1 = 250$, $\beta_1 = 750$, $\alpha_2 = 250$, $\beta_2 = 750$, (f) $\alpha_1 = 750$, $\beta_1 = 250$, $\alpha_2 = 250$, $\beta_2 = 750$, (g) $\alpha_1 = 250$, $\beta_1 = 750$, $\alpha_2 = 750$, $\beta_2 = 250$, (h) $\alpha_1 = 750$, $\beta_1 = 250$, $\alpha_2 = 750$, $\beta_2 = 250$. The order is limited to $m_{\max} = n_{\max} = 10$. (b), (c), and (d) show the cases where global features are extracted, i.e., $\alpha_1 = 0$, $\beta_1 = 0$, $\alpha_2 = 0$, $\beta_2 = 0$. In these cases, orders subject to (b) $m_{\max} = n_{\max} = 10$, (c) $m_{\max} = n_{\max} = 20$, and (d) $m_{\max} = n_{\max} = 30$ have been used. (i), (j), (k), and (l) show the Hahn moment kernels for $m = n = 1$ at different positions as determined by the parameters. Images (b), (c), (d), (e), (f), (g), and (h) are thresholded.

$$y_c = \frac{1}{N-1} \left(\sum_{x=0}^{M-1} \sum_{y=0}^{N-1} y f(x,y) \right) \left(\sum_{x=0}^{M-1} \sum_{y=0}^{N-1} f(x,y) \right)^{-1}. \tag{20}$$

Parameters $t_1(f)$ and $t_2(f)$ are to be selected in a global-local tradeoff manner described as follows: If we let $s_1(f)$ and $s_2(f)$ be measures determining the *spread* of the image object defined as

$$\begin{aligned} 0 \le s_1(f) &= \max[|x_c - x_{\min}|, |x_c - x_{\max}|] \le M - 1, \\ 0 \le s_2(f) &= \max[|y_c - y_{\min}|, |y_c - y_{\max}|] \le N - 1, \end{aligned} \tag{21}$$

where

$$\begin{aligned} x_{\min} &= \inf\{x | \exists y : f(x,y) \neq 0\}, \\ x_{\max} &= \sup\{x | \exists y : f(x,y) \neq 0\}, \\ y_{\min} &= \inf\{x | \exists x : f(x,y) \neq 0\}, \\ y_{\max} &= \sup\{x | \exists x : f(x,y) \neq 0\}, \end{aligned} \tag{22}$$

we can let $t_k(f) = a_k e^{b_k s_k(f)}$, where parameters a_k and b_k can be determined by using the following constraints: when $s_1(f) = 2\sigma_1 = 2\sqrt{M x_c (1 - x_c)}$, $t_1(f) = 20M$; when $s_1(f) = M - 1$, $t_1(f) = 0.01 \approx 0$; when $s_2(f) = 2\sigma_2 = 2\sqrt{N y_c (1 - y_c)}$, $t_2(f) = 20N$; and when $s_2(f) = N - 1$, $t_2(f) = 0.01 \approx 0$.

Some results using this adaptive scheme are shown in Fig. 5. It can be observed that Hahn moments adapt according to the location and size of the image object. To further the demonstrate the effectiveness of this scheme, we position the image object (an instance is shown in Fig. 5d) at 50 randomly selected locations and with adaptive Hahn moments extract the relevant information at the region of interest. The information extracted is again reflected by image reconstruction and the average MSE values are shown in Fig. 6. It can be observed that Hahn moments perform significantly better compared with the other moments in terms of reconstruction

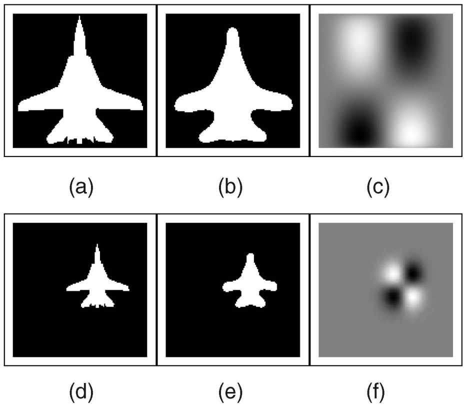

Fig. 5. Local feature extraction. Hahn moments adapt according to the location and size of the image object. (a) and (d) Original images, (b) and (e) reconstructed images (thresholded), and (c) and (f) moment kernels with $m = n = 1$. We have used $P = 10$ for all cases.

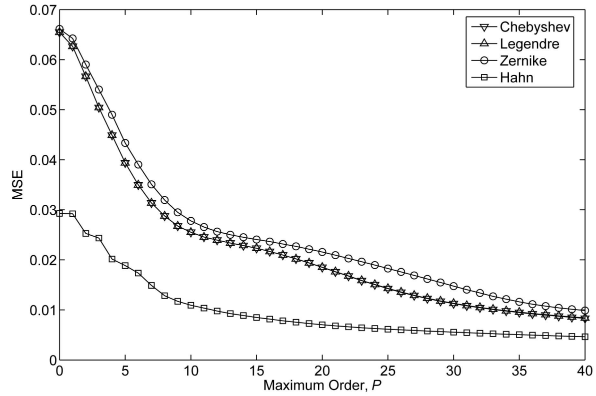

Fig. 6. MSE comparison of images reconstructed using Chebyshev, Legendre, Zernike, and adaptive Hahn moments, respectively. Note that the values for Chebyshev and Legendre moments are overlapped.

error. This provides the empirical proof that image information can be compacted in a lesser number of moment terms if the weight function is appropriately set to reflect the location of significance of the image. The weight function related to Hahn moments in this case gives more weight to the portion of the image which contains more relevant information and less weight to the portion of the image with less or discardable information.

5 Local Structure Analysis

The set of Hahn polynomials forms a complete basis in the weighted space defined by $w(x;\alpha,\beta,N-1)$. Since $w(x;\alpha,\beta,N-1)$, when $\alpha = \beta$ is a Gaussian like function which peaks in the middle and falls off toward the sides, Hahn polynomials can be adapted for local image analysis. The *normalized convolution* framework developed by Knutsson and Westin [6] is particularly well-suited for this purpose. The distinct advantage of normalized convolution is its concept of *Signal Certainty* philosophy [6], in which the both the data and the operator are separated into a signal part and a certainty part. This is especially useful in cases where the image data being dealt with is incomplete or is irregularly sampled. Incomplete data can be due to drop-outs or estimation problems in earlier processing stages. Using normalized convolution, the missing data can be simply handled by setting the certainty to zero in the corresponding certainty description and irregular sampling is handled by setting the certainty to one in the sampling points and zero elsewhere.

Let $\mathbf{f}$ denote the neighborhood of a given point of signal f. Assuming that the neighborhood is of finite size, $\mathbf{f}$ can be taken as an element of a vector space with finite dimension $\mathcal{C}^n$. Regardless of the dimensionality of the space, $\mathbf{f}$ is represented by an $n \times 1$ column vector. A set of basis functions, $\{\mathbf{b}_i\}_1^m \in \mathcal{C}^n$, can be chosen to give a local model for the signal. The set of basis functions can be collected as the column vectors of a $n \times m$ matrix $\mathbf{B}$. In the case where the basis function are linearly independent with respect to the norm $\|\cdot\|_{\mathbf{W}}$,[9] normalized convolution is at each signal point a question of finding a least square representation of the neighborhood $\mathbf{f}$:

$$\arg\min_{\mathbf{r}\in\mathcal{C}^m} \|\mathbf{Br}-\mathbf{f}\|_{\mathbf{w}} \tag{23}$$

and the solution of which is given by [6]

$$\mathbf{r} = (\mathbf{B}^H\mathbf{W}^2\mathbf{B})^{\dagger}\mathbf{B}^H\mathbf{W}^2\mathbf{f}, \tag{24}$$

where $(\cdot)^H$ denotes the Hermitian transpose. Signal interpolation utilizing normalized convolution is simply the process of finding a local model $\mathbf{Br}$ for each signal point and taking the middle point of the model as the interpolated value. Denoting $\mathbf{a}$ and $\mathbf{c}$ as the applicability function and signal certainty,[10] respectively, we can let the $n \times n$ matrices $\mathbf{W}_a = \mathrm{diag}(\mathbf{a})$ and $\mathbf{W}_c = \mathrm{diag}(\mathbf{c})$, and replace $\mathbf{W}^2$ with $\mathbf{W}_a\mathbf{W}_b$. In the current context, the set of 2D Hahn polynomials, $\{h_m(x;\alpha_1,\beta_1,M-1)h_n(y;\alpha_2,\beta_2,N-1)\}$, can be used as the basis function and the weight function $w(x;\alpha_1,\beta_1,M-1)w(y;\alpha_2,\beta_2,N-1)$ as the applicability function. We demonstrate the application of this scheme by performing, in the manner used in [6], interpolation of sparse *irregularly* sampled test image. The test image[11] shown in Fig. 7d is generated from Fig. 7a by gated white noise with the threshold chosen so that only 10 percent of the data remains. Attempts to reconstruct the image using simple smoothing operation are deemed to fail due to sample density variation, see Fig. 7b and Fig. 7c. On the other hand, normalized convolution compensates for the density variation effectively and, hence, gives far better results, as shown in Fig. 7e and Fig. 7f.

6 Conclusion

The concern of this paper is to show how Hahn moments provide a unified understanding of Chebyshev and Krawtchouk moments, and how this point can be exploited and utilized in the context of image analysis. The set of Hahn moments becomes Chebyshev moments or Krawtchouk moments depending on how the parameters $\{\alpha_1,\beta_1,\alpha_2,\beta_2\}$ are set, i.e., Chebyshev and Krawtchouk moments are particular cases of Hahn moments. A direct implication of this fact is that Hahn moments encompass all the properties of both Chebyshev and Krawtchouk moments, and Hahn moments, in addition, also exhibit intermediate properties between the extremes set by Chebyshev and Krawtchouk moments. This makes Hahn moments a unique set of feature descriptors in their own right. This paper aims to highlight the generalization property of Hahn moments and to show how this property can be properly exploited to make Hahn moments a useful set of image feature descriptors. In addition, we have also shown how Hahn moments can be

9. $\|\mathbf{v}\|_{\mathbf{W}} = \sqrt{(\mathbf{v},\mathbf{v})_{\mathbf{W}}} = \sqrt{(\mathbf{Wv},\mathbf{Wv})} = \|\mathbf{Wv}\|$.

10. Certainty gives the relative importance of the signal values in the least squares fit, while applicability gives the relative importance of basis functions and, hence, the points in the neighborhood.

11. We thank Corbis (pro.corbis.com) for this image.

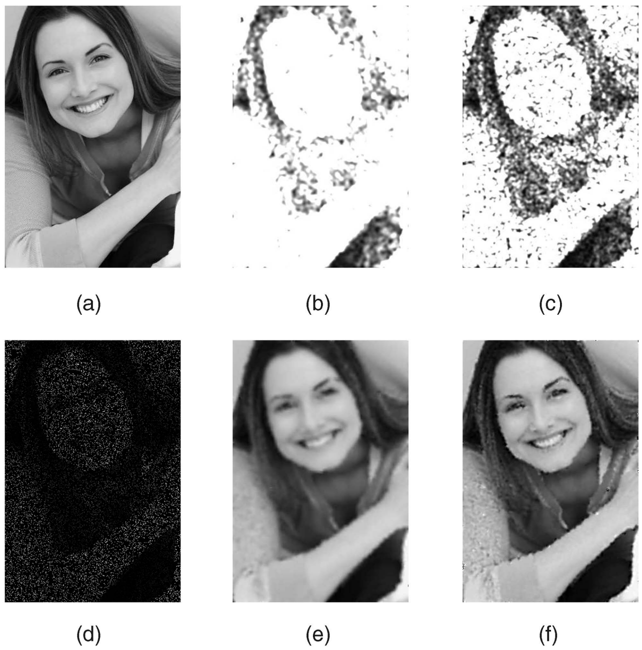

Fig. 7. Image interpolation. (a) Original image used for test. (d) The sampled test image containing only 10 percent of the original data. (b) Interpolation using standard convolution using the weight function of Hahn polynomials with $\alpha_1 = \beta_1 = \alpha_2 = \beta_2 = 5$ as the smoothing filter. (e) Interpolation using normalized convolution with the same filter in (b) as applicability function; the zeroth order $(m, n) = (0, 0)$ 2D Hahn polynomial is used. (c) Interpolation using standard convolution with a more local smoothing filter $(\alpha_1 = \beta_1 = \alpha_2 = \beta_2 = 50)$. (f) Normalized convolution using the same filter in (c) as applicability function and Hahn polynomials of higher order $(m, n) \in \{(0,0), (0,1), (1,0), (0,2), (2,0), (1,1)\}$.

incorporated into the framework of normalized convolution to analyze local structures of irregularly sampled signals. This is build upon the fact that the set of Hahn polynomials spans a weighted space defined by the related weight function, which for the case of Hahn polynomials resembles the Gaussian function.

REFERENCES

[1] R. Mukundan, S.H. Ong, and P.A. Lee, "Image Analysis by Tchebichef Moments," *IEEE Trans. Image Processing,* vol. 10, no. 9, pp. 1357-1364, Sept. 2001.

[2] P.-T. Yap, R. Paramesran, and S.-H. Ong, "Image Analysis by Krawtchouk Moments," *IEEE Trans. Image Processing,* vol. 12, no. 11, pp. 1367-1377, Nov. 2003.

[3] P.-T. Yap, "Image Analysis by Discrete Orthogonal Moments," master's thesis, Univ. of Malaya, Kuala Lumpur, Malaysia, Apr. 2003.

[4] P.-T. Yap, "Moments-Based Pattern Analysis: Theory and Applications," PhD dissertation, Univ. of Malaya, Kuala Lumpur, Malaysia, 2006.

[5] J. Zhou, H.Z. Huazhong Shu, C. Toumoulin, and L. Luo, "Image Analysis by Discrete Orthogonal Hahn Moments," *Proc. Second Int'l Conf. Image Analysis and Recognition,* p. 524, Sept. 2005.

[6] H. Knutsson and C.-F. Westin, "Normalized and Differential Convolution: Methods for Interpolation and Filtering of Incomplete and Uncertain Data," *Proc. IEEE CS Conf. Computer Vision and Pattern Recognition,* pp. 515-523, June 1993.

[7] W. Hahn, "Über Orthogonalpolynome, Die q-Differenzengleichungen genügen," *Math. Nachrichten,* vol. 2, pp. 4-34, 1949.

[8] G.H. Golub and C.F.V. Loan, *Matrix Computations,* third ed. The Johns Hopkins Univ. Press, 1996.

[9] E. Kreyszig, *Advanced Engineering Mathematics,* sixth ed. John Wiley & Sons, 1988.

[10] J.Z. Wang, G. Wiederhold, O. Firschein, and S.X. Wei, "Content-Based Image Indexing and Searching Using Daubechies' Wavelets," *Int'l J. Digital Libraries,* pp. 311-328, 1997.

[11] M.R. Teague, "Image Analysis via the General Theory of Moments," *J. Optical Soc. Am.,* vol. 70, no. 8, pp. 920-930, Aug. 1980.